AD-A010 480

IGNITION PHASE BLAST FIELD STUDY

John Erdos, et al

Advanced Technology Laboratories, Incorporated

Prepared for:

Air Force Office of Scientific Research

April 1975

SECURITY CLASSIFICATION OF THIS PAGE (When Data Entered)

REPORT DOCUMENTATION PAGE		READ INSTRUCTIONS BEFORE COMPLETING FORM
1. REPORT NUMBER AFOSR - TR - 75 - 0714	2. GOVT ACCESSION NO.	3. RECIPIENT'S CATALOG NUMBER AD-A010 480
4. TITLE (and Subtitle) IGNITION PHASE BLAST FIELD STUDY		5. TYPE OF REPORT & PERIOD COVERED INTERIM 15 Jan 1974-14 Jan 1975
		6. PERFORMING ORG. REPORT NUMBER ATL TR 211
7. AUTHOR(s) JOHN ERDOS JOHN RANLET		8. CONTRACT OR GRANT NUMBER(s) F44620-74-C-0041
9. PERFORMING ORGANIZATION NAME AND ADDRESS ADVANCED TECHNOLOGY LABORATORIES, INC MERRICK AND STEWART AVENUES WESTBURY, NEW YORK 11590		10. PROGRAM ELEMENT, PROJECT, TASK AREA & WORK UNIT NUMBERS 681308 9711-01 61102F
11. CONTROLLING OFFICE NAME AND ADDRESS AIR FORCE OFFICE OF SCIENTIFIC RESEARCH/NA 1400 WILSON BOULEVARD ARLINGTON, VIRGINIA 22209		12. REPORT DATE April 1975
		13. NUMBER OF PAGES 30
14. MONITORING AGENCY NAME & ADDRESS(if different from Controlling Office)		15. SECURITY CLASS. (of this report) UNCLASSIFIED
		15a. DECLASSIFICATION/DOWNGRADING SCHEDULE

16. DISTRIBUTION STATEMENT (of this Report)

Approved for public release; distribution unlimited.

17. DISTRIBUTION STATEMENT (of the abstract entered in Block 20, if different from Report)

18. SUPPLEMENTARY NOTES

19. KEY WORDS (Continue on reverse side if necessary and identify by block number)
UNSTEADY FLOWS
BLAST WAVES
SHOCK WAVES AND DETONATION
ROCKET IGNITION

20. ABSTRACT (Continue on reverse side if necessary and identify by block number)

Evolution of the ignition phase blast field of a tube or silo launched rocket is described in terms of three distinct phase or steps. The first or precursor phase is associated with leakage of the high pressure gas (termed the launch gas) used to eject the rocket from the tube. The second phase occurs when the bulk of the launch gas is released as the rocket base clears the end of the tube. Both these steps are analogous to their counterparts in the muzzle blast of a conventional gun. However, the third, and probably most severe, phase in the subject problem accompanies ignition of the rocket motor and initial production

DD FORM 1 JAN 73 1473 EDITION OF 1 NOV 65 IS OBSOLETE

UNCLASSIFIED
SECURITY CLASSIFICATION OF THIS PAGE (When Data Entered)

of thrust. The present report describes work performed on two facets of the subject problem. The first is analysis of the internal gas flow during start of the launch. Particular attention is given to formation of the salient characteristics of the flow field which will affect the precursor phase of the blast field. Results of several numerical examples are presented to illustrate the properties of the internal flow field. The second facet of the problem which has been studied is the ignition-phase blast field, per se. Initial development of the field is described in terms of cylindrically symmetric and spherically symmetric approximations. Numerical results are presented to illustrate the qualitative character of the initial inviscid development of the blast field; however caution must be exercised in quantitative interpretation of the results as the model is highly idealized. The importance of turbulent mixing and buoyant transport of the propellant exhaust gases during the later stages is pointed out.

APRIL 1975

ATL TR 211

IGNITION PHASE BLAST FIELD STUDY

By

John Erdos and John Ranlet

INTERIM SCIENTIFIC REPORT

FOR PERIOD OF

JANUARY 15, 1974 THROUGH JANUARY 14, 1975

UNDER

CONTRACT NO. F44620-74-C-0041

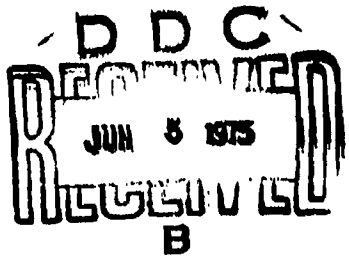

BY

ADVANCED TECHNOLOGY LABORATORIES, INC.
Merrick and Stewart Avenues
Westbury, New York 11590

III

INDEX

LIST OF FIGURES

LIST OF SYMBOLS

A	cross-sectional area of gas flow passage
A_b	cross-sectional area of vehicle base
a	speed of sound
C_p	specific heat at constant pressure
g	acceleration of gravity
p	pressure
p_b	pressure on vehicle base
r	radial distance from launch axis
S	entropy
T	temperature
t	time
u	gas velocity
u_p	vehicle velocity
W_p	vehicle weight
x	distance along launch axis
x_b	position of vehicle base
γ	ratio of specific heats
η	distance from base, $x-x_b$
ϕ	launch angle, measured from vertical

ABSTRACT

Evolution of the ignition phase blast field of a tube or silo launched rocket is described in terms of three distinct phases or steps. The first or precursor phase is associated with leakage of the high pressure gas (termed the launch gas) used to eject the rocket from the tube. The second phase occurs when the bulk of the launch gas is released as the rocket base clears the end of the tube. Both these steps are analogous to their counterparts in the muzzle blast of a conventional gun. However, the third, and probably most severe, phase in the subject problem accompanies ignition of the rocket motor and initial production of thrust.

The present report describes work performed on two facets of the subject problem. The first is analysis of the internal gas flow during start of the launch. Particular attention is given to formation of the salient characteristics of the flow field which will affect the precursor phase of the blast field. Results of several numerical examples are presented to illustrate the properties of the internal flow field. The second facet of the problem which has been studied is the ignition-phase blast field, per se. Initial development of the field is described in terms of cylindrically symmetric and spherically symmetric approximations. Numerical results are presented to illustrate the qualitative character of the initial inviscid development of the blast field; however caution must be exercised in quantitative interpretation of the results as the model is highly idealized. The importance of turbulent mixing and buoyant transport of the propellant exhaust gases during the later stages is pointed out.

SECTION I
INTRODUCTION

The presently considered ignition phase blast field is associated with launch of a rocket from a tube using compressed air or a gas generator. Ignition of the rocket motor is assumed to occur after the exhaust nozzle has cleared the muzzle end of the tube. The breech end of the tube is assumed to be closed (i.e., separate vents are not considered). The general configuration is indicated in Figure (1), which is based on published information on the Sprint interceptor system. The important physical characteristics of the assumed configuration which bear on the internal flow of the launch gas and the resulting external blast field, and distinguish the subject problem from internal ballistics of conventional guns, are:

(a) The launch tube is approximately the same length as the vehicle.

(b) The diameter of the launch tube may be slightly larger than the maximum diameter of the vehicle.

The blast field generated by this type launch is believed to occur in three fairly distinct phases or steps, of increasing intensity. The first is a precursor phase associated with escape of the launch gas around the vehicle prior to its emergence from the tube. The second phase is the blast field produced when the bulk of the launch gas is released as the base of the vehicle (or the point of maximum diameter) passes the open end of the tube. The third, and probably most intense, phase occurs when the rocket motor is ignited and thrust is sustained.

The gas dynamics of the first two phases is analogous to that of the blast field produced by conventional guns (cf. References 1 and 2), although the precursor phase in the present case is associated with gas leakage rather than expulsion of the column of gas from a long gun tube. In particular, the approximation of a spherically symmetric field can be expected to produce a reasonably accurate rendition of the principal features of the expanding shock layer between the leading blast wave and the Mach disc which terminates the exhaust

plume. However, the third phase in evolution of the blast field, which is associated with rocket motor ignition, is dissimilar from the first two in several important respects. In addition to the important differences in the thermochemical properties of the rocket motor exhaust gas compared to the launch gas, the ignition-generated blast field is directed back toward the launch tube and will reflect off the ground plane, as in the case of an underground silo for example. In this case, after the initial reflection off the ground, the pressure field may grow in a roughly cylindrical fashion and then evolve into a hemispherical field. Expansion of the cloud of rocket exhaust gases will occur on a somewhat slower time scale than propagation of the blast overpressure, and its behavior is much more difficult to model, since it will be dominated at later times by turbulent motion and buoyant forces. However, at early times it may be possible to describe it by an inviscid expansion.

The effort to date has addressed two facets of the subject problem, viz. description of the internal gas flow during the launch phase, and preliminary modelling of the ignition generated blast field in the vicinity of a ground plane.

SECTION II

INTERNAL GAS FLOW DURING LAUNCH

Production of a volume of high pressure gas in the breech cavity at the time of launch is assumed to be accomplished instantaneously by ignition of an explosive charge, bursting of a diaphragm, or a similar mechanism. Thereafter, the volume of the breech cavity expands as the vehicle accelerates in accord with the standard ballistic formula:

$$\frac{du_p}{dt} = g\left[\frac{p_b A_b}{W_p} - \cos\phi\right] \qquad (1)$$

The variation of pressure and temperature in the breech cavity could probably be adequately described by the classical Lagrangian model, i.e., a homogeneous isentropic expansion, if the loss of gas around the sides of the vehicle due to highly imperfect obturation were negligible. The gap between the vehicle base (or point of maximum diameter) and the tube walls forms a gas-dynamic throat which controls the rate of loss of gas from the breech cavity, but the loss is not assumed to be negligible. The escaping gas will drive a shock into the ambient air in the launch tube, which upon emergence from the tube forms the precursor blast wave. In addition, under the conditions of expanding area in the launch tube due to a tapered vehicle shape such as indicated in Figure (1), the escaping gas will accelerate to supersonic speed and a second shock will form. Therefore, emergence of the escaping launch gas from the tube will be preceded by a slug of shock-heated air. The launch gas will also be shock-heated, until the second shock passes out of the tube and thereafter it may be expected to continue exhausting in a cool, supersonic state. This precursor phase will be terminated when the vehicle base or throat reaches the muzzle of the launch tube.

Development of a quantitative model of the internal gas flow during the precursor phase has proceeding along the lines described in Reference (3), viz. an unsteady, one-dimensional flow analysis with variable cross-sectional area. However, the formulation described in Reference (3) has been extended to include representation of the geometric throat as an area discontinuity. The various possible jump conditions pertaining to such an area discontinuity are discussed in Reference (4)

with respect to a stationary configuration. In the present case, however, the location of the area discontinuity will translate with the vehicle velocity, u_p. Therefore, the jump conditions have been reformulated in a coordinate system translating with the vehicle velocity.

The Mach number-area relationship across the discontinuity is given by:

$$\frac{MA}{\left(1 + \frac{\gamma-1}{2} M^2\right)^{\frac{\gamma+1}{2(\gamma-1)}}} = \text{constant} \qquad (2)$$

The compatibility relations on the upstream and downstream travelling waves are:

$$\frac{d \ln p}{dt} \pm \frac{\gamma}{a} \frac{du}{dt} = - \left(\frac{\partial \ln A}{\partial t} + u \frac{\partial \ln A}{\partial x}\right) \qquad (3)$$

on $\quad \frac{dx}{dt} = u \pm a \quad .$

The energy equation is:

$$\frac{dS}{dt} = 0 \qquad \text{on} \qquad \frac{dx}{dt} = u \qquad (4)$$

Integrated forms of Equations (3) and (4) together with Equation (2) and the constraint that the total pressure is invariant across the jump provide a complete system for determination of the instantaneous conditions on each side of the area discontinuity, given a set of initial conditions.

It should be pointed out that only four (4) combinations of flow conditions entering and exiting the area discontinuity are possible:

(a) subsonic flow in - subsonic flow out
(b) subsonic flow in - sonic flow out
(c) supersonic flow in- sonic flow out
(d) supersonic flow in- supersonic flow out

Thus a transition from supersonic to subsonic flow entering the discontinuity can only occur through a shock wave, which must be treated separately. In the context of the subject problem, only subsonic flow entering the discontinuity (from the breech cavity) is anticipated.

Initial conditions at the start of launch are estimated by employing a shock-tube type analysis, including, however, the area discontinuity and assuming sonic flow out of the breech cavity. Thus, the initial conditions include a leading shock moving downstream from the throat, a contact surface separating the launch gas from the ambient air (also moving downstream from the throat), and an expansion fan moving upstream into the breech cavity.

A finite-difference method, as described in Reference (3), is used to describe the flow in the breech cavity and throughout the launch tube. The leading shock, the contact surface, the throat (area discontinuity) and the closed (breech) end of the breech cavity form boundaries of three (3) domains which are spanned by separate finite-difference grid networks. Details of the method are discussed in Reference (3), although in the previous work only two (2) domains were considered and the area discontinuity was treated as a continuous variation.

Two numerical examples have been carried out for the configuration sketched in Figure (1). A vertical launch has been considered, using a gas compressed to 22.3 atmospheres. This pressure level was selected to give a 100g vehicle acceleration for an assumed vehicle weight of 7500 lb. The initial gas temperature in the breech was taken as 5260°R. In this sense the conditions simulate an explosive charge of conventional gun propellant; however the gas is assumed to have the molecular weight of air. A constant ratio of specific heats, $\gamma = 1.25$, was used for the launch gas, and $\gamma = 1.40$ was used for the ambient air in the tube. This calculation was terminated at an elapsed time of approximately 1500 μsec, at which time formation of the salient gas-dynamic features of the flow field were clearly evident. The vehicle had acquired a velocity of 4.5 fps, but had barely moved. Therefore, a second hypothetical example was carried out for a vehicle weight of only 75 lb. to exaggerate the effect of vehicle acceleration (i.e., 10^4 g's). In this case the vehicle reaches velocity of 300 fps

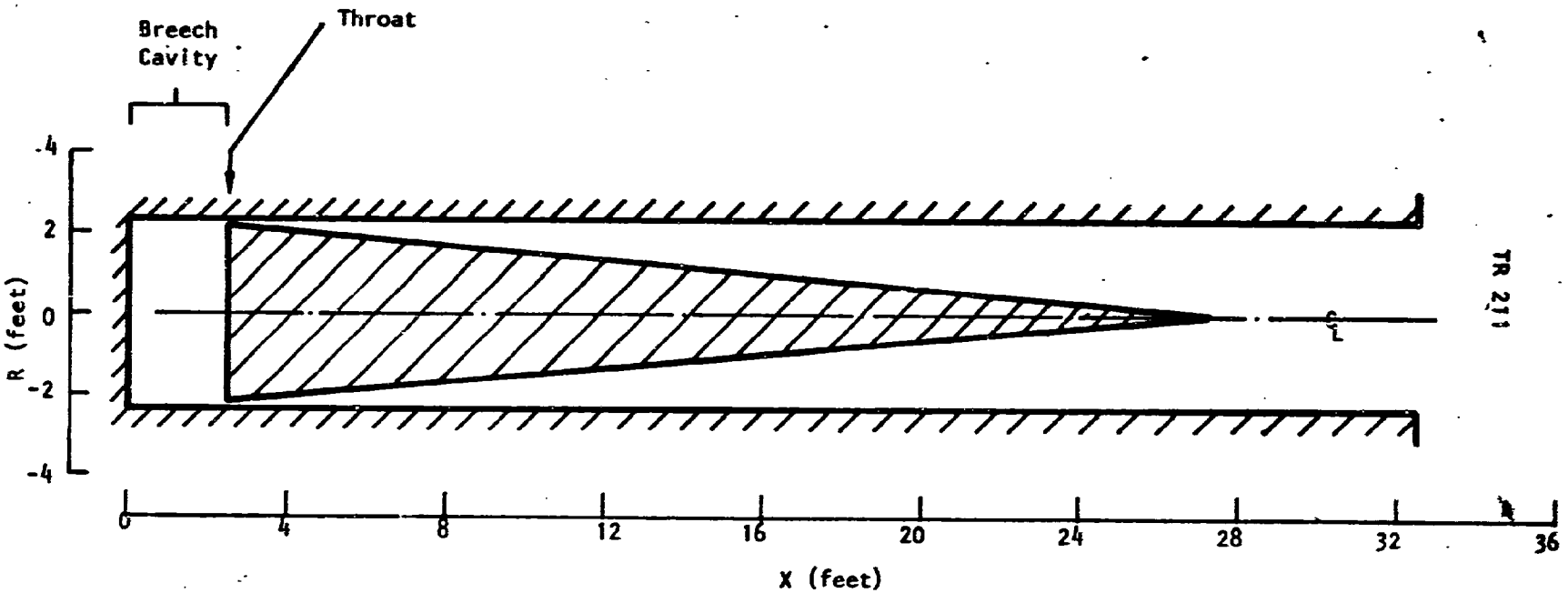

FIGURE 1. GENERAL CONFIGURATION OF SPRINT-TYPE LAUNCH TUBE AND VEHICLE

in 1000 μsec.

As can be seen in Figure (2), the effect of vehicle motion on the rate of propagation of the leading shock wave and of the contact surface is extremely slight on the considered time scale in these examples. Since the contact surface velocity represents the frontal velocity of the escaping launch gas, it is evident that the vehicle velocity is only of the order of 0.1% of the contact velocity in the first example and about 1% in the second and therefore negligible in both cases. The effect of vehicle velocity will become appreciable by the time the vehicle leaves the tube in the second case (the 75 lb. vehicle), but should be negligible during the entire launch in the first case (the 7500 lb. vehicle).

Formation of a second shock in the period between 200 and 800 μsec is indicated by the gas velocity distributions shown as a function of distance from the vehicle base in Figure (3). The points labelled S and C refer to the positions of the leading shock and the contact surface, respectively. The second shock is "captured" numerically by the finite-difference solution; its position at time step 300 is indicated by the steep gradient between $1.0 < \eta < 1.1$ ft. A comparison of the gas velocity distributions for the two vehicle weights is shown in Figure (4). Since these are shown as a function of distance from the vehicle base, the positions of the shocks and contacts are displaced; they are virtually coincident in terms of actual position in the tube. Corresponding distributions of pressure and temperature are displayed in Figures (5) and (6). The presence of shock heated air ($T \underset{\sim}{>} 1150^{\circ}R$) driven ahead of the contact surface and shock heated launch gas ($T \underset{\sim}{>} 4160^{\circ}R$) following the contact is evident in the latter figure.

The first example (the 7500 lb. vehicle) was terminated at 1460 μsec and the second example (the 75 lb. vehicle) was terminated at 1010 μsec, since the salient features of the internal gas flow were evident by these times. Execution times on a CDC 7600 computer system were 25 seconds and 11 seconds, respectively. The computation times grow as the distance covered by the leading shock increases, due to a mesh control provision which maintains a prescribed maximum grid size by adding grid points as necessary. Use of a fixed number of

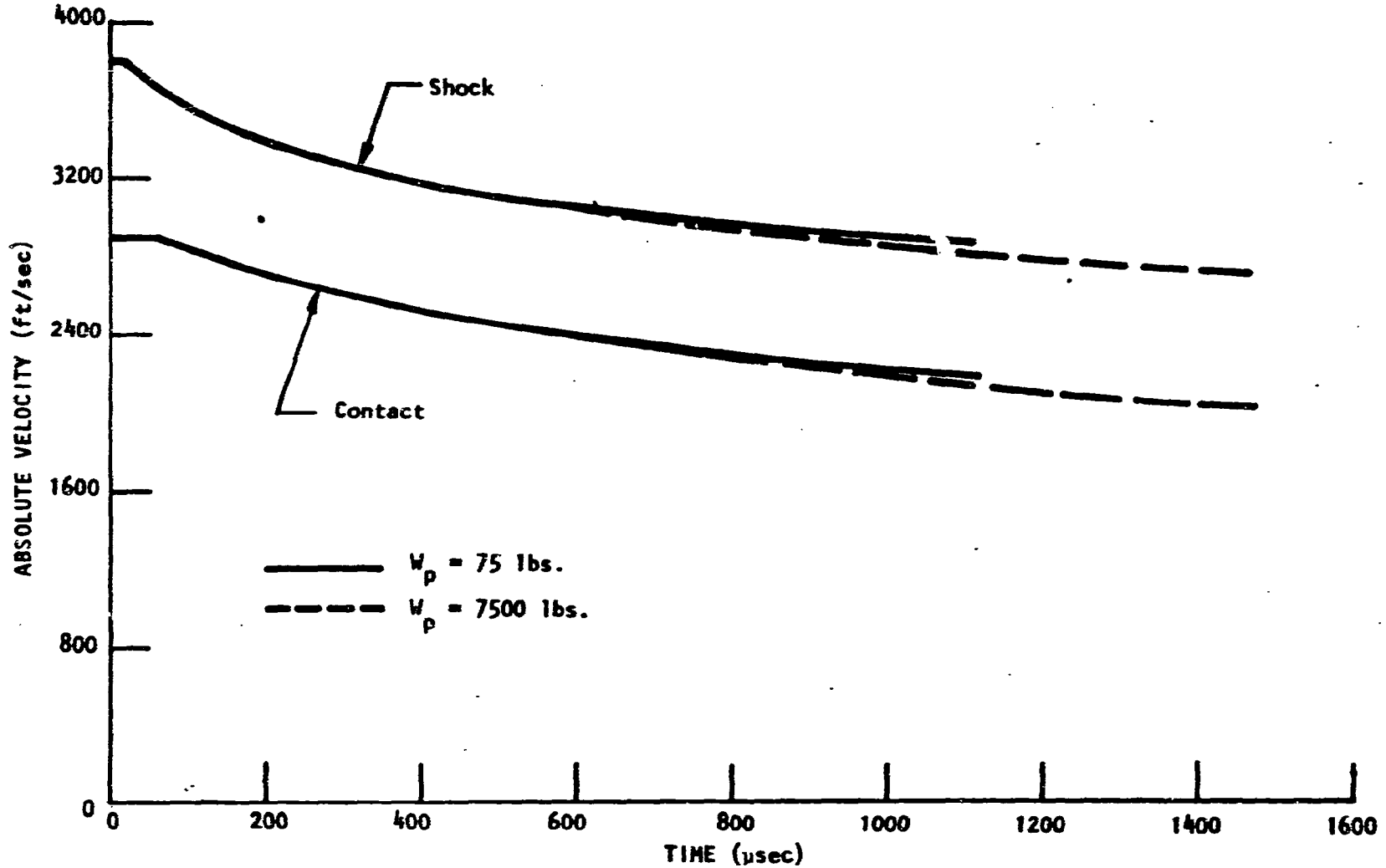

FIGURE 2. VELOCITY OF LEADING SHOCK WAVE AND OF CONTACT SURFACE AS A FUNCTION OF TIME

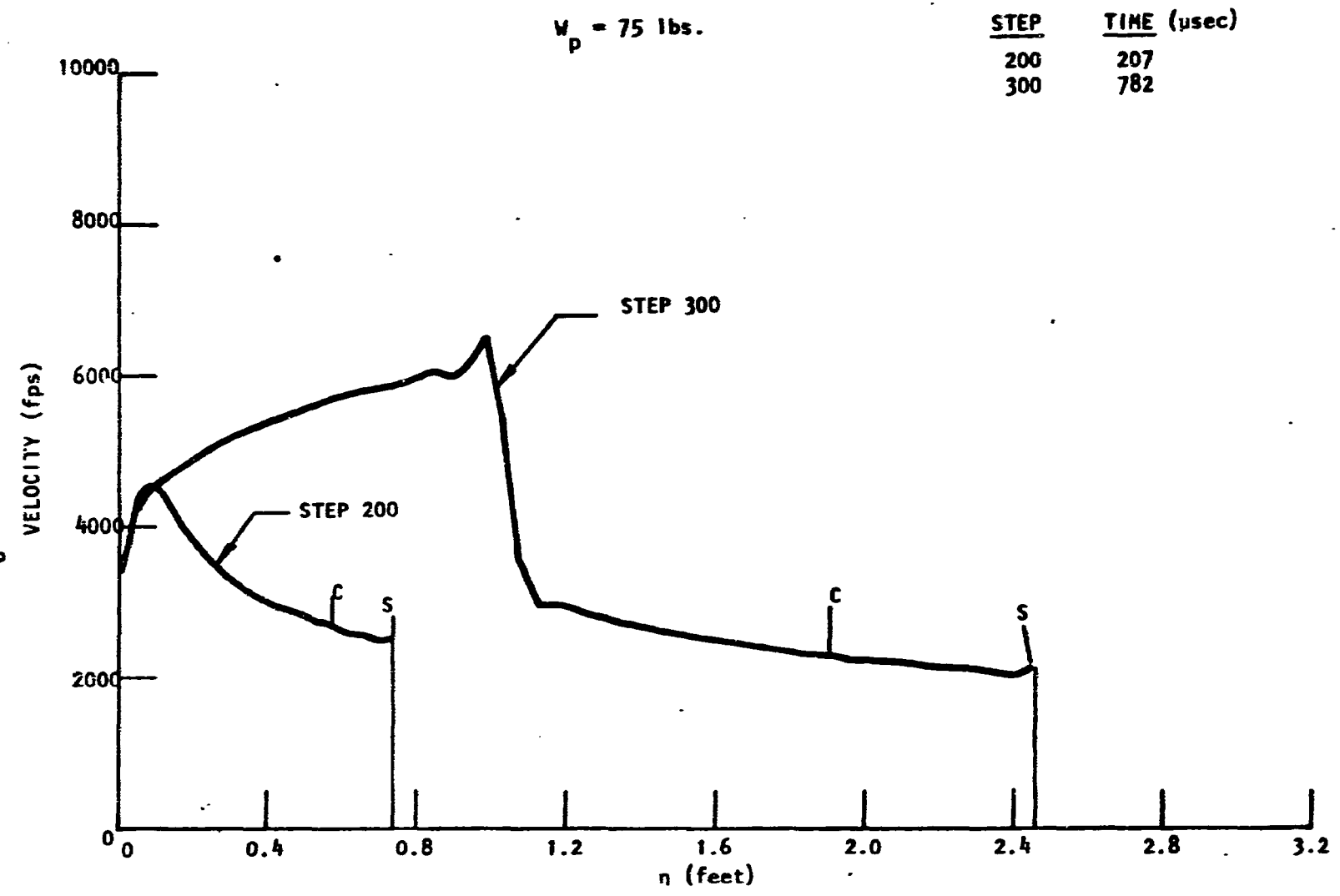

FIGURE 3. GAS VELOCITY DISTRIBUTIONS AT TIME STEPS 200 AND 300

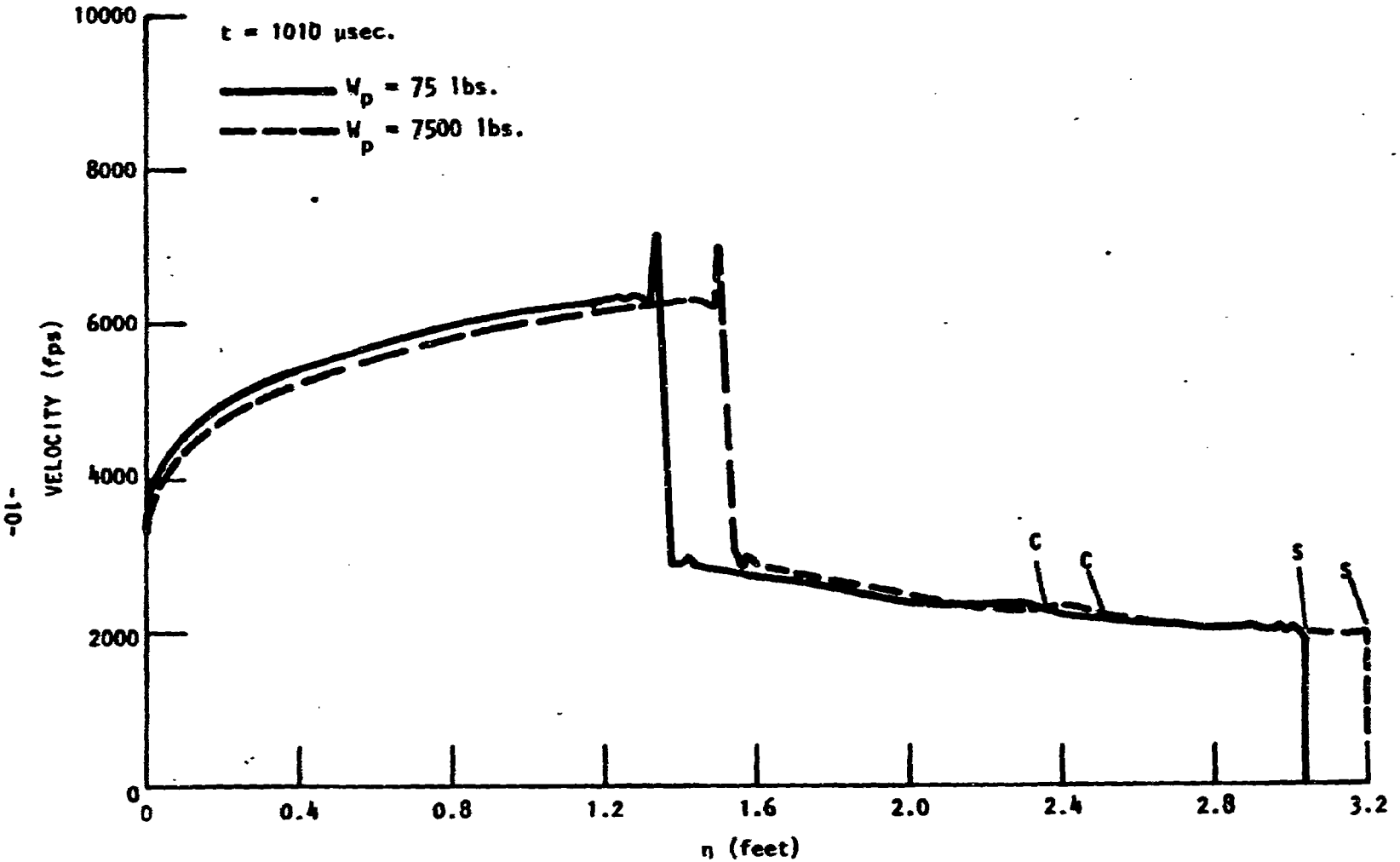

TR 211

FIGURE 4. COMPARISON OF GAS VELOCITY DISTRIBUTIONS AT TIME = 1010 μsec

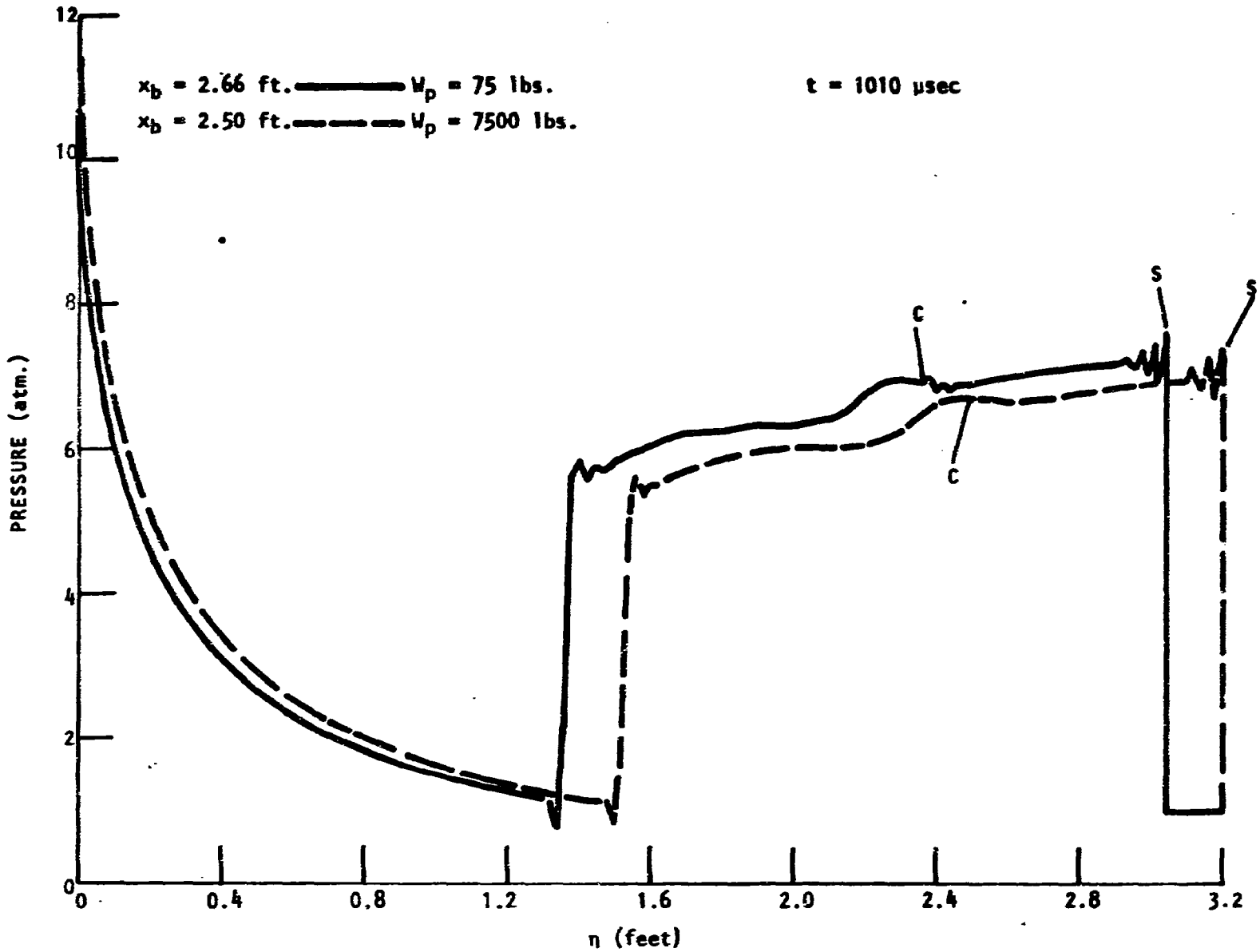

FIGURE 5. COMPARISON OF PRESSURE DISTRIBUTION AT TIME = 1010 μsec

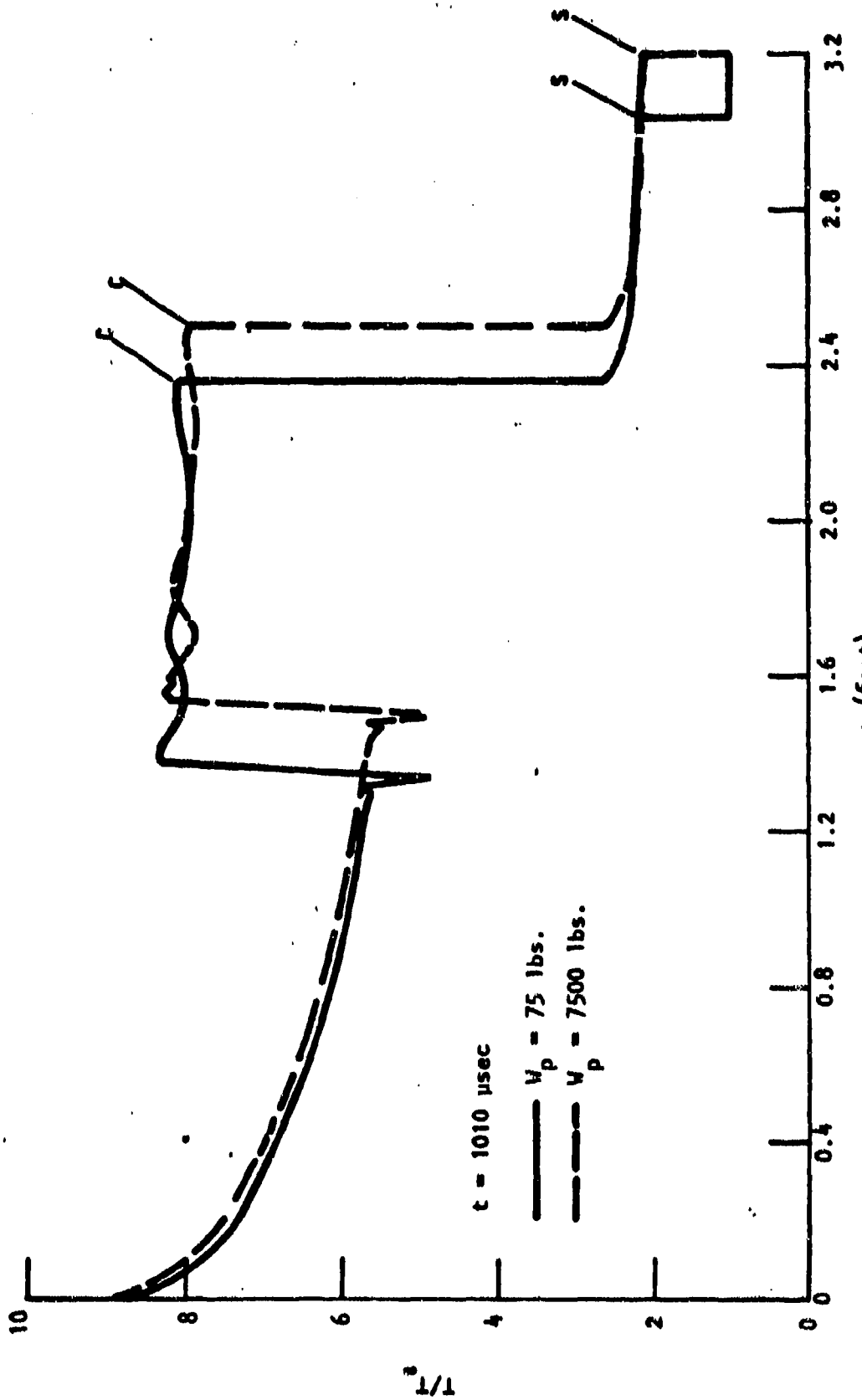

FIGURE 6. COMPARISON OF TEMPERATURE DISTRIBUTIONS AT TIME = 1010 μsec.

grid points allows the permissible time step to increase in proportion to the increase in grid size as the distance between the bounding surfaces of discontinuity grows; however the accompanying deterioration in numerical accuracy has been found to be unacceptable. Therefore, continuation of the calculations for the entire launch period is feasible, but the cost was not considered to be warranted for the present exploratory study.

SECTION III

IGNITION PHASE BLAST FIELD

As indicated in the introductory remarks, the third phase in the blast field evolution, namely, the ignition-generated blast, is probably the most severe vis-a-vis overpressure, visible flash and smoke, and the most difficult to model. In addition to the obvious complexity of describing the thermochemical state of the propellant gases, the gas-dynamic flow field is highly three-dimensional and eventually dominated by buoyant transport of a vortex ring ("smoke ring") and turbulent mixing. However, some insight regarding the initial, inviscid stage of development of the ignition blast field has been gained by application of the concepts and methodology pertaining to more conventional muzzle blast fields.

A sketch of the main features of an idealized model of the ignition-phase blast field is shown in Figure (7). The tube exit is assumed to be coincident with the ground surface, the flight path is assumed to be vertical, and the vehicle velocity is small compared to the rate of propagation of the blast wave. The effects of the launch gas escaping from the tube are neglected, including the interaction between the blast field associated therewith and the presently considered ignition phase blast field. Ignition is assumed to occur at a small distance above the ground and produces a supersonic plume which expands radially outward along the ground. At very early times after ignition the blast field should possess cylindrical symmetry with respect to the flight axis, under the assumed conditions, as indicated on the left-hand side of Figure (7). Near the ground plane the variations normal to the ground can be neglected as a first approximation. However, the blast wave will subsequently become spherically symmetric, as indicated on the right-hand side of this figure. Variations in flow properties normal to the ground plane will become more significant, but, again to a first approximation, spherical symmetry can be ascribed to the entire blast field. Obviously these are idealized approximations which yield a tractable one-dimensional, unsteady flow problem, whereas the actual blast field will be two-dimensional at best and highly three-dimensional if the flight axis is not precisely vertical.

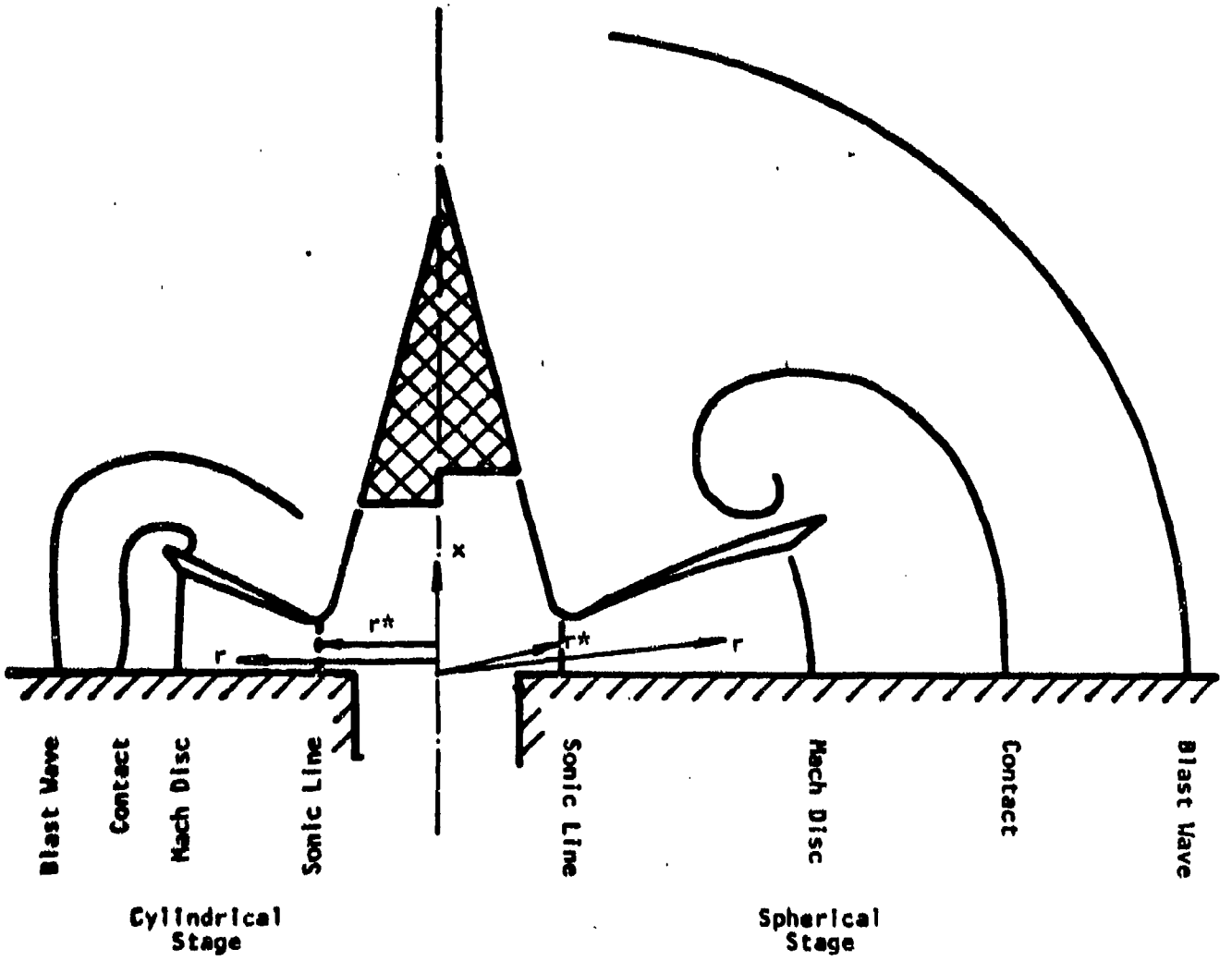

FIGURE 7. SKETCH OF IDEALIZED MODEL OF IGNITION PHASE BLAST FIELD

A cylindrically symmetric blast field has been calculated for a rocket motor having a chamber pressure of 35 atmospheres and a chamber temperature of 8350°R. The propellant gas is assumed to have $\gamma = 1.25$ and $C_p = 8580.\ ft^2/sec^2/°R$ (i.e., the same molecular weight as air). The supersonic plume Mach number distribution has been calculated for a steady cylindrically symmetric source flow. The trajectories of the blast wave, contact surface and Mach disc are shown in Figure (8), as functions of scaled distance and time. The radial distance has been scaled with respect to the distance to the sonic line, r^*, and time with respect to the speed of sound at the sonic line, a^*, and r^*. The value of a^* is 4000 fps in this case. To verify that these are indeed the appropriate scale factors and that the procedure for establishing initial conditions for a blast field (discussed in Reference 5) is consistent with this scaling, calculations have been executed with values of r^* which differ by a factor of ten. However, as pointed out in Reference (1), this scaling will only pertain for the same chamber pressure and for a constant rate of energy addition, as assumed in this calculation.

A comparison of the trajectories of the blast wave, contact and Mach disc for spherically and cylindrically symmetric flow fields is presented in Figure (9). A noticeable decrease in the velocities of all three surfaces is evident in the spherical case, relative to the cylindrical case, as should be expected. Unfortunately no reliable estimate can be made á priori for the transition of the actual blast field from a cylindrical-like flow to a spherical-like flow. However, it is noted that at early times, i.e., $ta^*/r^* < 4$, there is relatively little difference between the two solutions and, therefore, it is likely that the transition will occur in this initial period.

To illustrate the character of the blast field, distributions of pressure, temperature and gas velocity at $ta^*/r^* = 12$ are shown in Figures (10), (11) and (12). It may be noted that although the blast wave produces the maximum overpressure in the shock layer (i.e., between the Mach disc and blast wave), the temperature rise produced by the blast wave is quite insignificant compared to that produced by the Mach disc. The region between the Mach disc and contact surface contains a volume of propellant exhaust gases at temperatures not substantially less than

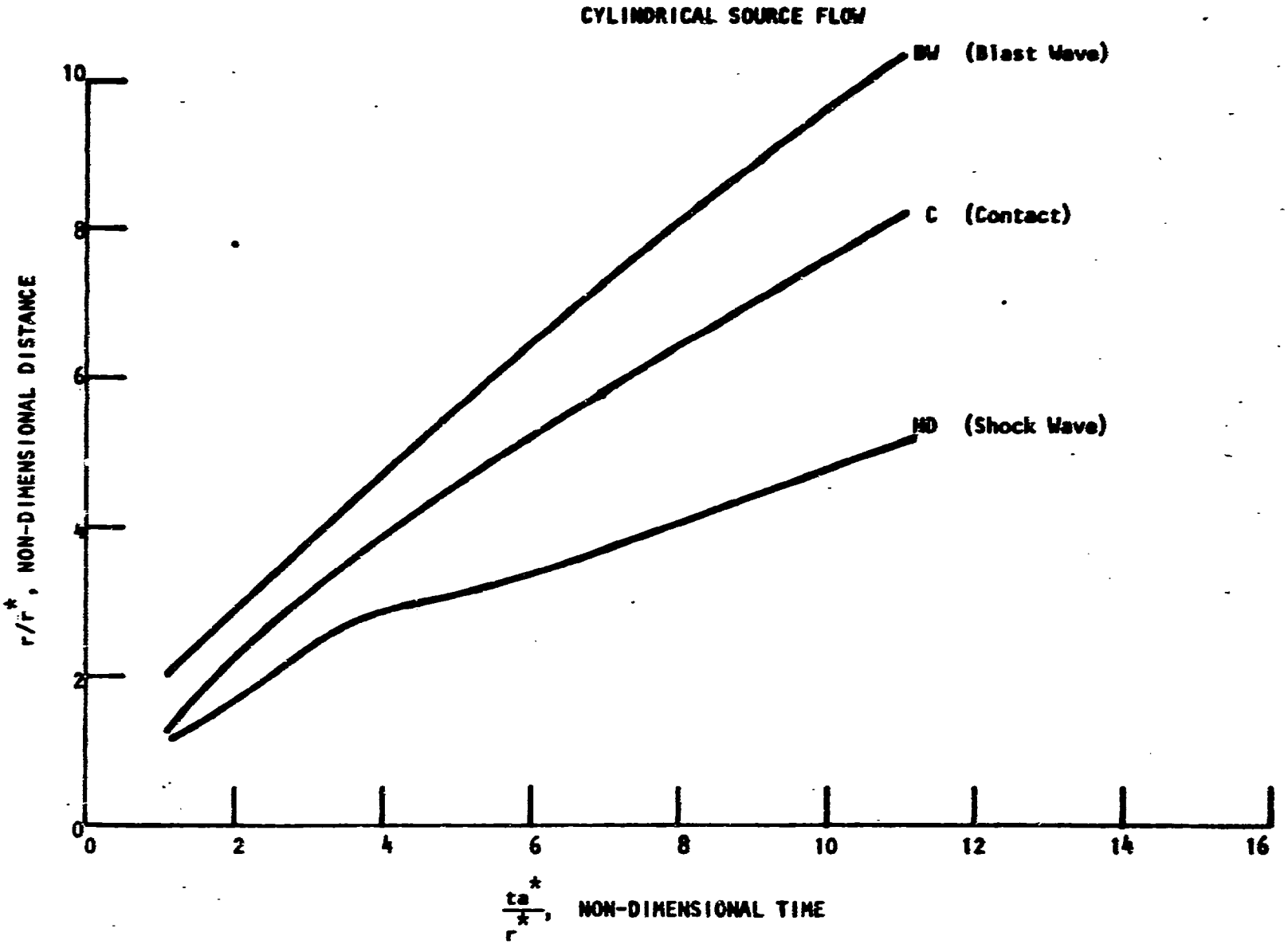

FIGURE 8. BLAST WAVE CONTACT AND MACH DISC TRAJECTORIES FOR A CYLINDRICAL BLAST FIELD

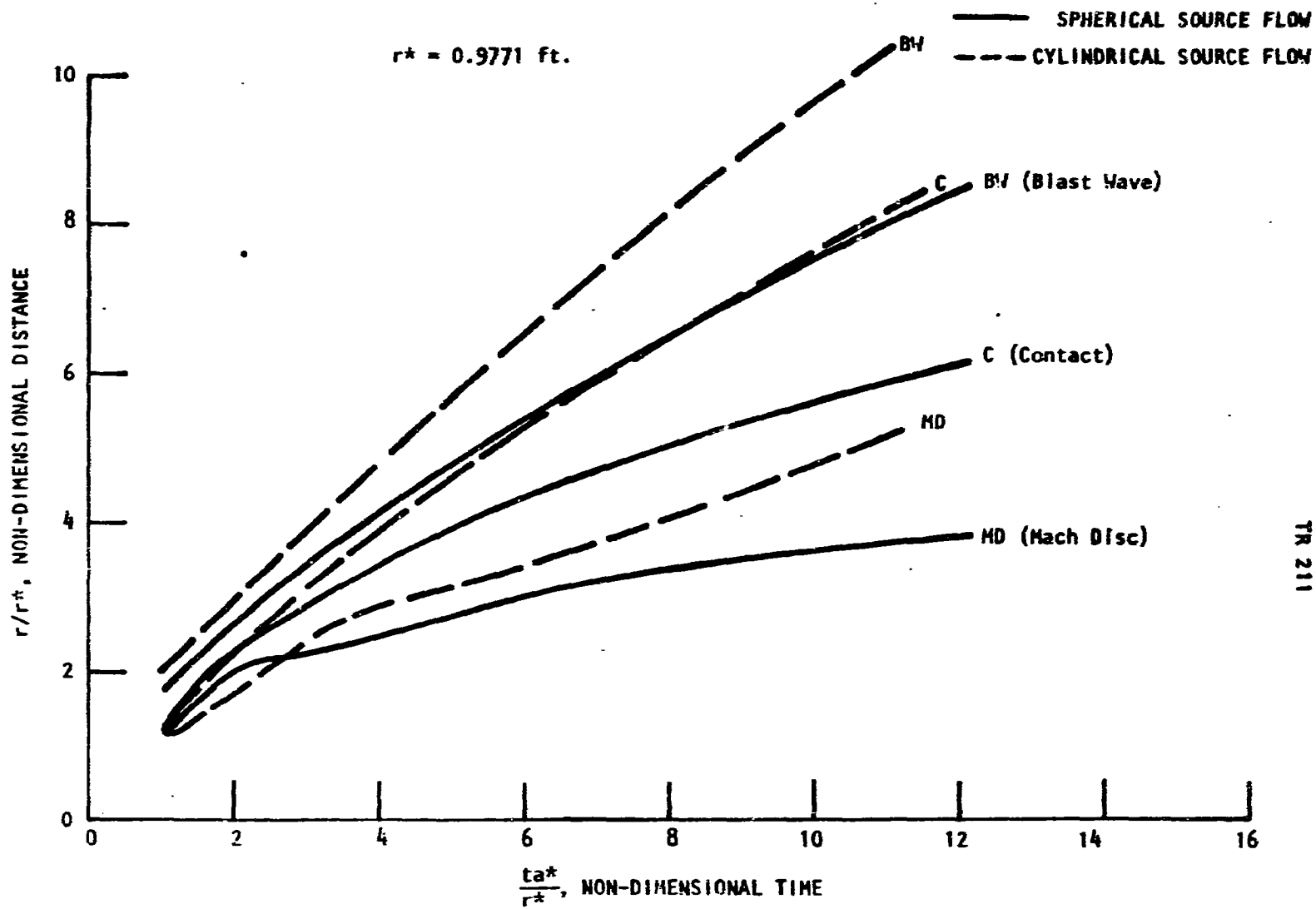

FIGURE 9. COMPARISON OF BLAST WAVE, CONTACT AND MACH DISC TRAJECTORIES FOR SPHERICAL BLAST AND CYLINDRICAL BLAST FIELDS

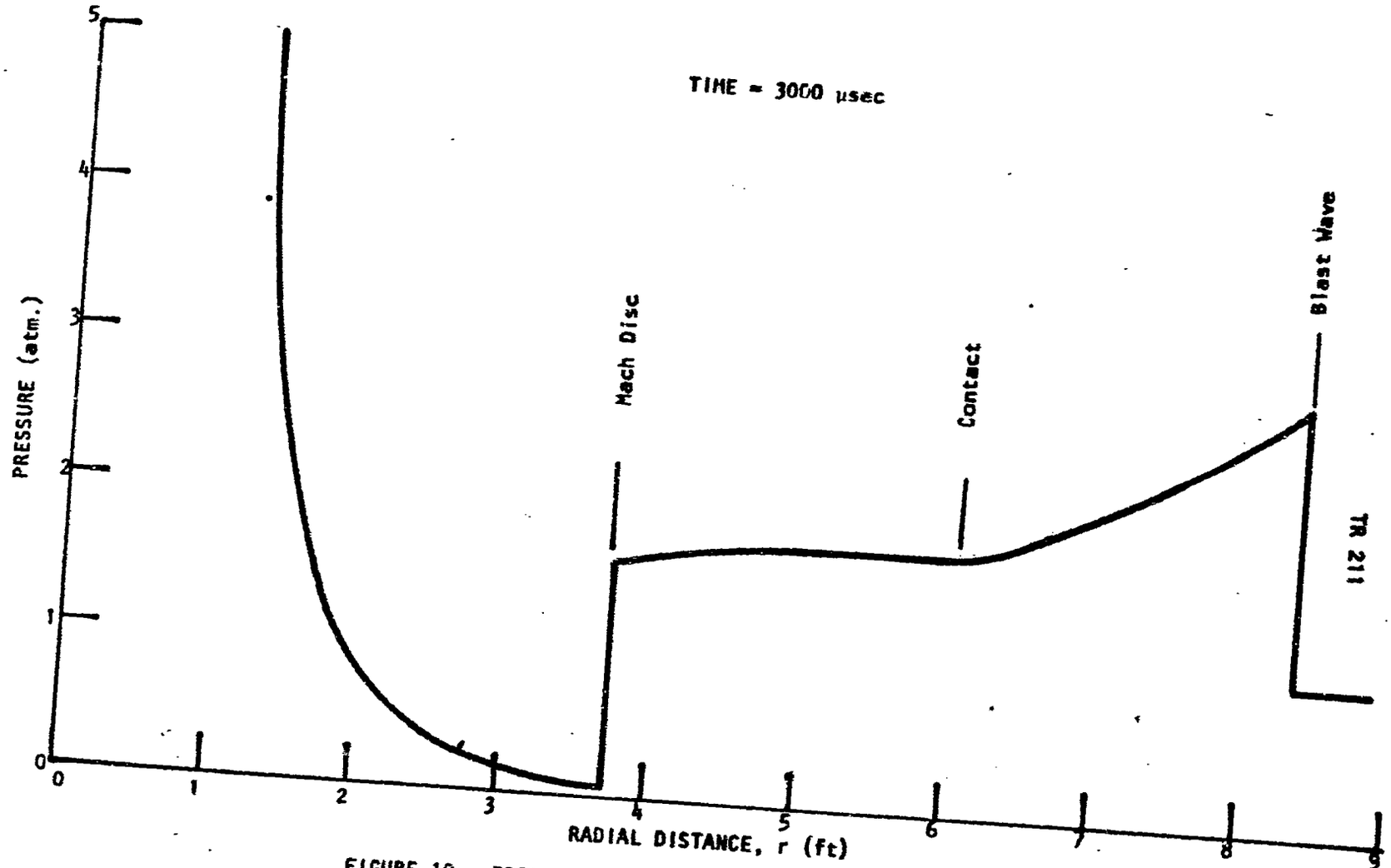

FIGURE 10. PRESSURE DISTRIBUTION IN SPHERICAL BLAST FIELD

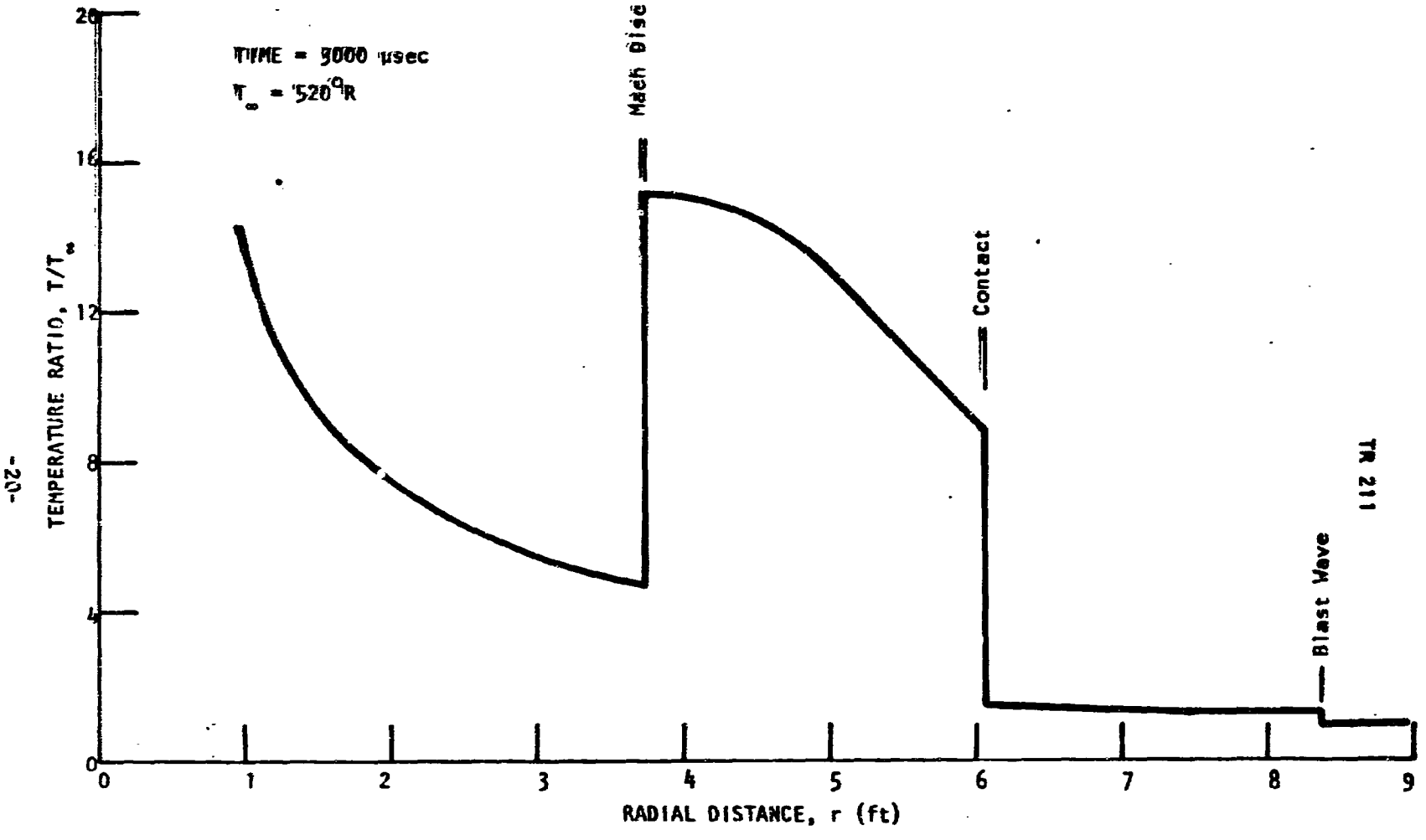

FIGURE 11. TEMPERATURE DISTRIBUTION IN SPHERICAL BLAST FIELD (FROZEN GASES)

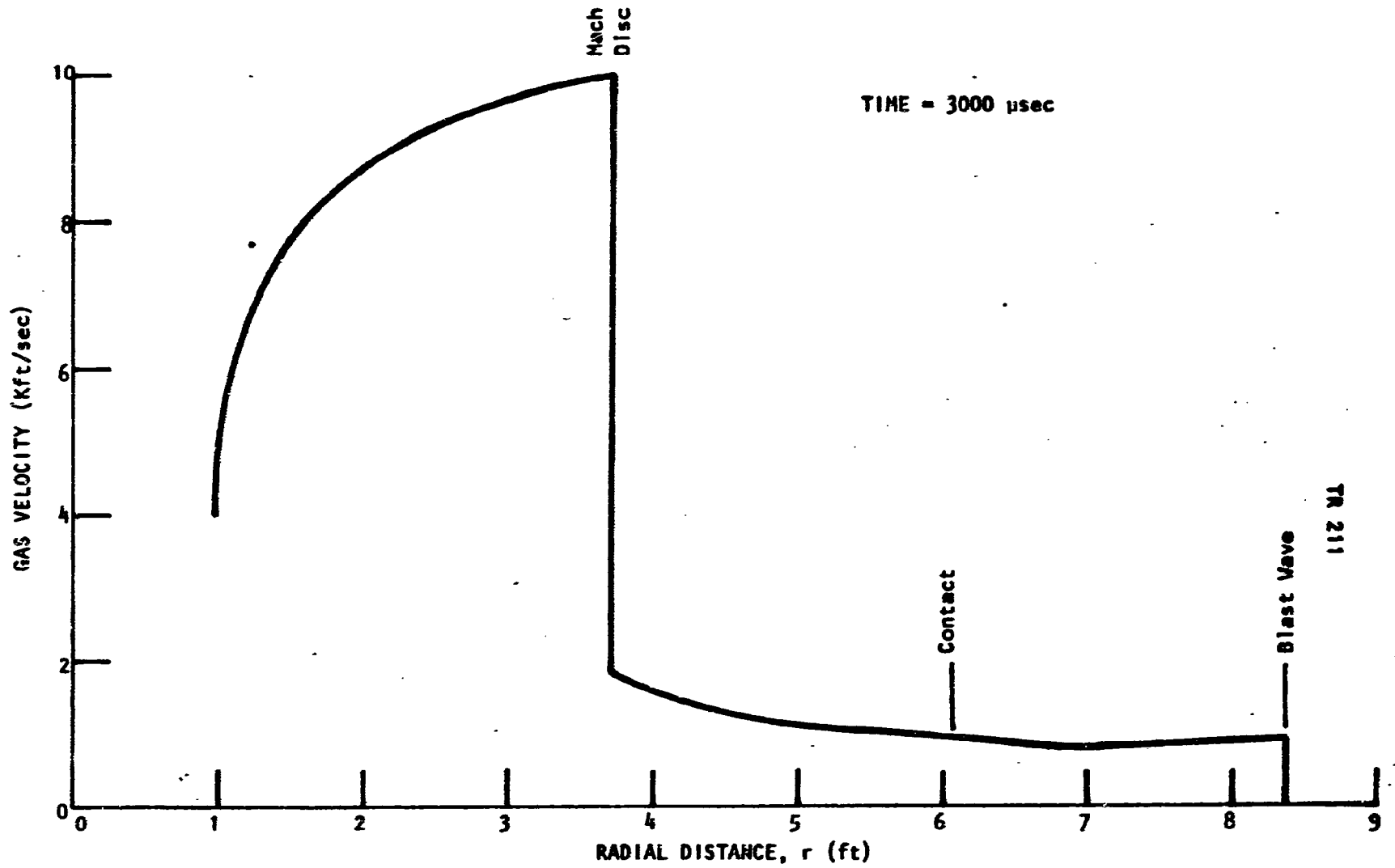

FIGURE 12. GAS VELOCITY DISTRIBUTION IN SPHERICAL BLAST FIELD

those in the combustion chamber. The gas in this region will initially be cooled by expansion as the volume grows, but eventually turbulent mixing will predominate. It should also be pointed out that the gas density in this region is less than 1/5 of atmospheric density at 3 milliseconds, and although it will increase as the gas cools, buoyant forces may be expected to increasingly contribute the motion of this volume of gas as the inertial forces decay.

SECTION IV
CONCLUSIONS

The ignition phase blast field associated with launch of a rocket from a tube occurs in three steps: a precursor phase, a launch phase and an ignition phase. The precursor phase represents the loss of high pressure gas used for the launch due to imperfect seal between the rocket and the tube walls. The launch phase corresponds to release of the launch gas as the rocket clears the tube exit. The ignition phase occurs upon ignition of the rocket motor outside the tube. The present study has addressed two facets of the subject problem. The first is description of the internal gas flow during launch with a view toward exposition of the salient features of the gas dynamic processes affecting the precursor and launch phases of the blast field. The second is description of the ignition phase blast field, per se.

Two numerical examples have been carried out for launch of a Sprint-type vehicle. In the first case conditions were selected which produce a 100g initial acceleration of the vehicle. The main features of the flow field are established within the first 1500 μsec. Since the vehicle velocity is negligible in this case, a second case having a hundred-fold decrease in vehicle weight to produce a 10^4g acceleration was considered. The vehicle velocity was again found to have negligible effect on development of the flow field structure, although some quantitative influence could be expected by the time the vehicle cleared the tube exit in this case. Particular attention is called to the shock which forms within the escaping launch gas, as well as that driven ahead of the gas in the ambient air. The shock-heated air will be driven out of the tube first, followed by escaping shock-heated launch gas. The gas following the second shock should exhaust as a cool, supersonic stream, until the vehicle base clears the tube exit and the bulk of the launch gas is released.

The ignition phase blast field has been described in terms of cylindrically symmetric and spherically symmetric one-dimensional approximations. A comparison of the rates of propagation of the blast wave, contact surface and Mach disc

associated with cylindrical and spherical fields has been presented. It is suggested that the transition of the actual blast field from a cylindrical-like flow to a spherical-like flow should occur at a non-dimensional time of $ta^*/r^* < 4$. Calculated distributions of flow properties in the spherical blast field at $ta^*/r^* = 12$ indicate that the region between the contact surface (i.e., the front of the propellant exhaust gases) and the Mach disc contains gases at temperatures not substantially below the combustion chamber temperature. This region will initally cool as the volume expands but turbulent mixing will eventually predominate. It is also pointed out that buoyant forces will increasingly contribute to the motion of this volume of exhaust gas as the inertial forces decay. Therefore, a more complete model of the ignition phase blast field should be at least two-dimensional (if not three-dimensional) and include representation of the effects of turbulent mixing and buoyant transport of the exhaust gases at late times.

REFERENCES

1. Erdos, J. and Del Guidice, P., "Calculation of Muzzle Blast Flow Fields," to appear in AIAA Journal. Also see "Gas Dynamics of Muzzle Blast" AIAA Paper No. 74-532, June 1974.

2. Schmidt, E. and Shear, D., "Experimental Study of Muzzle Blast Flow Fields," to appear in AIAA Journal. Also see "Formation and Decay of Impulsive, Supersonic Jets" AIAA Paper No. 74-531, June 1974.

3. Erdos, J. and Ranlet, J., "Analysis of a Muzzle Gas Venting Scheme," BRL CR No. 215, March 1975. Also issued as ATL TR 197, March 1974.

4. Napolitano, L., "Flows with Discontinuities," Chapter II in "Fundamental Data Obtained from Shock Tube Experiments" A. Ferri, Editor, AGARDograph No. 41, Pergamon Press, N. Y. 1961.

5. Erdos, J. and Ranlet, J., 2nd Quarterly Report prepared under Contract DAAD05-74-C-0784, submitted to BRL, Aberdeen Proving Ground, Md., February 1975.